



Possibilities and Limitations of ALE Large Deformations Analyses in Geotechnical Engineering

Frank Rackwitz^(✉)

Chair of Soil Mechanics and Geotechnical Engineering, Technische Universität
Berlin, Gustav-Meyer-Allee 25, 13355 Berlin, Germany
frank.rackwitz@tu-berlin.de

Abstract. A number of geotechnical engineering problems involve large deformations in the soil. While small deformation geotechnical problems can be adequately analyzed by means of conventional Lagrangian FEM, such an approach exhibits considerable shortcomings when the soil undergoes significant deformation. Hence methods have been developed which overcome these shortcomings. Among the methods using a computational mesh, the most promising approaches include the ALE methods: Coupled Eulerian-Lagrangian (CEL) method, the Simplified or Single-Material Arbitrary Lagrangian-Eulerian (SALE) method, and the Multi-Material Arbitrary Lagrangian-Eulerian (MMALE) method. In this contribution the possible advantages and limitations of ALE in comparison to other numerical approaches are presented. The performance of ALE methods is evaluated by means of two application examples. First the vibratory driven installation of open-ended tubular steel piles in sand is modeled and local large deformation due to initial pile imperfections and soil heterogeneity is analyzed. Second the sand column collapse problem is simulated using different modeling approaches and soil models as well. Simulation results assess the feasibility of ALE methods in geotechnical large deformation problems. It can be concluded that the ALE method could be considered as a promising framework for solving complex large deformation problems in geotechnical engineering.

1 Introduction

The Finite Element Method (FEM) is probably the most widely used numerical approach for solving boundary value problems in geotechnical engineering. The traditional formulations of FEM are based on either the Lagrangian or the Eulerian viewpoint. In the Lagrangian formulation the mesh deformation coincides with the material deformation, where the material can be the soil or a structure. In the Eulerian formulation the mesh is fixed and the movement of the material is independent of the mesh. The conventional Lagrangian FEM approach exhibits considerable limitations when the soil undergoes significant, large deformation. Methods that overcome the limitations of classical FEM can be divided into two groups: mesh-based and mesh-free or point (particle)-based (such as the material point methods (MPM) [1] and smoothed

particle hydrodynamics (SPH [2]) approaches as well. Figure 1 gives an overview of the continuum based approaches in use.

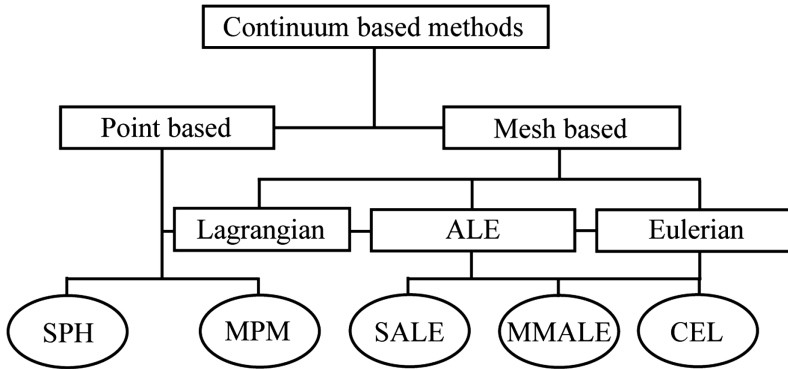


Fig. 1. Overview of the continuum based approaches for the analysis of large deformation problems

The most promising mesh-based approaches include the Coupled Eulerian-Lagrangian (CEL) method, the Simplified or Single-Material Arbitrary Lagrangian-Eulerian (SALE) method, and the Multi-Material Arbitrary Lagrangian-Eulerian (MMALE) method. Irrespective of the method used, the material behavior of the soil shall be described by a suitable non-linear constitutive model. Also the behavior of the interface between the soil and the structure, if it exists in the problem, has to be modeled adequately. Both mentioned requirements complicate the formulation and implementation of the chosen approach.

There are commercial as well as freely available programs, the latter primarily developed at universities for use in research. Not every program contains all the methods listed above. In addition to that there are two well known general strategies to solve the algebraic systems of discretized finite element equations: implicit and explicit solution procedures. Implicit solution procedures are based on the control of the equilibrium of forces and of the error of the solution variables. This makes it possible to control and achieve the convergence of the solution. But at the same time this has a disadvantage due to the need for a convergent solution in any case. In explicit solution procedures there is no such control, instead a minimal time step size has to be used to achieve a reliable solution. It leads to a high number of time steps compared to the same problem solved by an implicit scheme, but the need for a convergent solution is not an issue. A comprehensive comparison of different approaches has to consider the mentioned details of modeling aspects and solution procedures. In this way, the possibilities and limits of the approaches can be demonstrated.

2 ALE Methods

Due to the difficulties and restrictions occurring from the simply Lagrangian and Eulerian approaches when simulating large deformation problems, a more general approach was called for. The arbitrary Lagrangian–Eulerian (ALE) method has been developed in order to overcome these limitations and to combine the advantages of the purely Lagrangian and Eulerian approaches [3]. In an ALE method the computational mesh is regarded as an independent reference domain. The ALE mesh can be continuously smoothed so that the element quality is maintained until the end of the calculation. Mesh connectivity is kept unchanged hence the solution variables can be mapped to the improved mesh by means of advection algorithms. The most general approach within the ALE framework is referred to as MMALE – Multi-Material ALE – which means, that there can be more than one material within a finite element. In addition to the general method, some simplifications have been developed. One simplification allows only one material in a finite element and it is named SALE – Single-Material or Simplified ALE. Another specialization resigns any mesh update, i.e. a fixed Eulerian mesh is used throughout the analysis and this method is called CEL. The CEL method links overlapping but otherwise independent Lagrange and Euler meshes. An edge of the structure discretized with a Lagrange mesh usually forms the contact surface for the connection of the two independent meshes.

All above mentioned approaches are schematically drawn in Fig. 2 illustrating a Lagrangian modeled structure, such as a pile or foundation, penetrating into a deforming material, such as soil.

In recent years the CEL approach has been often used to solve large deformation geotechnical problems [5–8]. Qui et al. [5] analyze a strip footing, pile penetration, and ship grounding problem by means of CEL. Penetration of a jack-up spudcan foundation into seabed was investigated by Qui and Henke [6] and Tho et al. [7]. Hamann et al. [8] investigated the pile installation process into fully saturated soil under partially drained conditions.

After the ALE method had reached a certain level of development and application in the engineering sciences [3], first applications in geomechanics were made by Di et al. [9]. They developed an ALE method where the soil is modeled as a saturated porous material with solid–fluid coupling and strong material non-linearity. Later Aubram et al. [10] investigated a strip footing as well as a monotonic pile penetration problem into sandy soil by means of a SALE model. Recently Aubram et al. [11] provided the theoretical background and basis of development of ALE methods for modeling of vibro-pile penetration problems into sandy soils by means of the MMALE approach.

3 Practical Applications

The possibilities and limitations of the methods are best revealed in the analysis of real applications where large soil deformations occur. From the variety of possible applications, two are selected and analysed in the following sections. First, a current problem is investigated in connection with the dynamic installation of open tubular

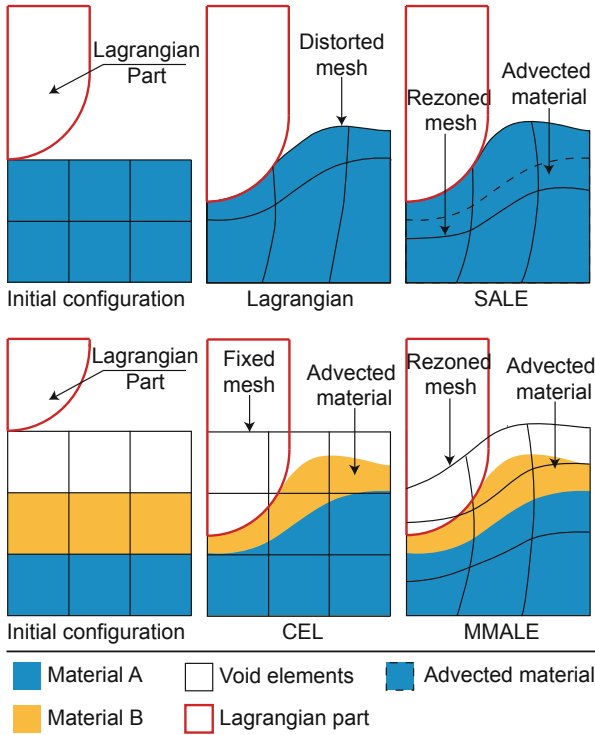


Fig. 2. Illustration of different FEM modeling approaches with respect to mesh and material deformation [4]

steel piles into soil. The second application example is the numerical simulation of a laboratory experiment in which a sand column flows out of a hollow cylinder opened at the bottom. The comparison between numerical and experimental results allows a validation of the calculation model. All numerical analyses have been performed using the commercial code LS-DYNA by means of explicit solution techniques.

3.1 Steel Pipe Buckling During Installation

A numerical model has been developed simulating a pile installation into soil by means of vibratory forces. The finite element model, dimensions and vibratory loading with time are shown in Fig. 3. The model pile has dimensions height/outer diameter/wall thickness = 1.5/0.2/0.005 m. The pile is modeled using the conventional Lagrangian element formulation with single point reduced integration and a uniform element size of 2 cm (3,000 elements). An elastic-perfectly plastic material model based on the von Mises failure criterion is used for the pile with the material properties density 7,850 kg/m³, Young's modulus 2.1E5, Poisson's ratio 0.3 and Yield stress 250 MPa. The pile head is fixed against horizontal movements.

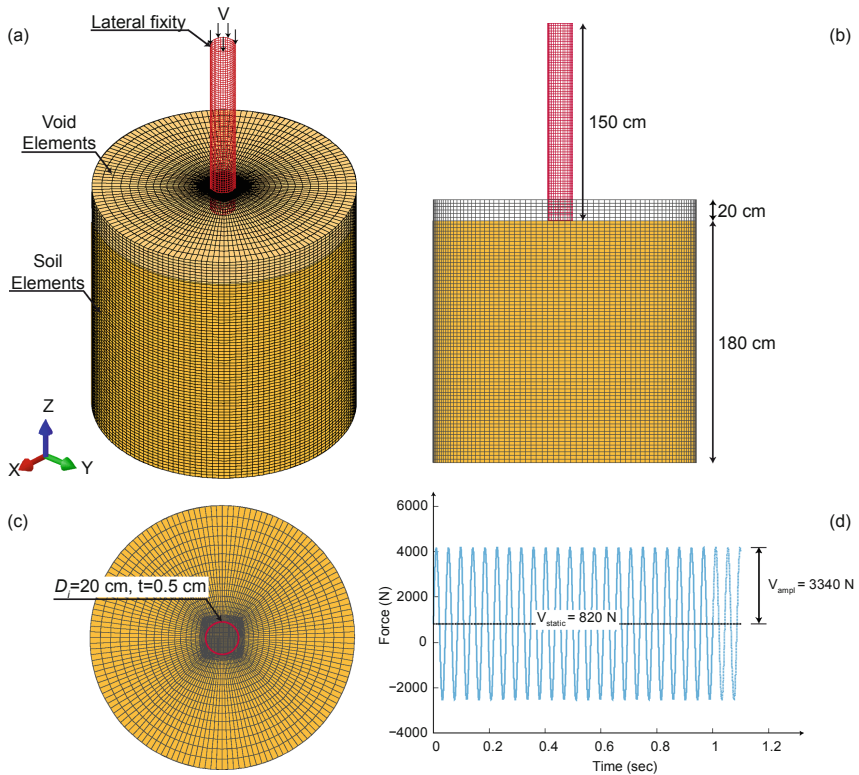


Fig. 3. FE model of pipe pile installation: (a) isometric, (b) side, and (c) planar view, and (d) vibratory loading time function [12]

The overall soil and void volume with 2 m height and 1 m radius is discretized by means of MMALE element formulation using one-point integration with in total 367,200 elements. The void domain with 0.2 m height, which has neither mass nor strength, was defined above the soil material to enable the soil to move to this domain during penetration of the pile. The lateral sides of the soil are constrained against movements in a direction perpendicular to their faces, while fixity in all directions is applied to the bottom of the soil.

A simple Mohr-Coulomb constitutive equation is used to capture the Berlin sand behavior in the model with parameters density $1,900 \text{ kg/m}^3$, friction angle 35° , dilatancy angle 1° , cohesion 1 kPa, Young's modulus 20 MPa and Poisson's ratio 0.2. The initial stress state in the soil is prescribed using the gravity acceleration of 10 m/s^2 . Penalty contact between the Lagrangian pile elements and the MMALE soil elements is defined with a tangential friction coefficient of 0.1. The equipotential smoothing technique is applied where the computational grids are rearranged to maintain the mesh quality [13]. For the ALE advection step, the 2nd-order accurate van Leer method is chosen [14].

The proposed numerical model is successfully validated by back-calculating an experimental test carried out in the laboratory of the author. The test set-up consists of a half-cylindrical pile with 1.5 m length, 0.005 m wall thickness, and 0.2 m outer diameter as well as a chamber with three rigid steel walls and one glass panel. The pile is fixed in the horizontal direction via pile guides to ensure penetration along the glass panel. A vibratory motor produces the driving force of 1,670 N with the frequency of 23 Hz. The imposed dead load on the pile is about 410 N. The chamber is filled with Berlin sand. The pile is modeled as rigid in this analysis. Figure 4 illustrates the resulting normalized displacement curve obtained from the numerical model and compared with experimental measurements from the model test. The overall agreement is very good.

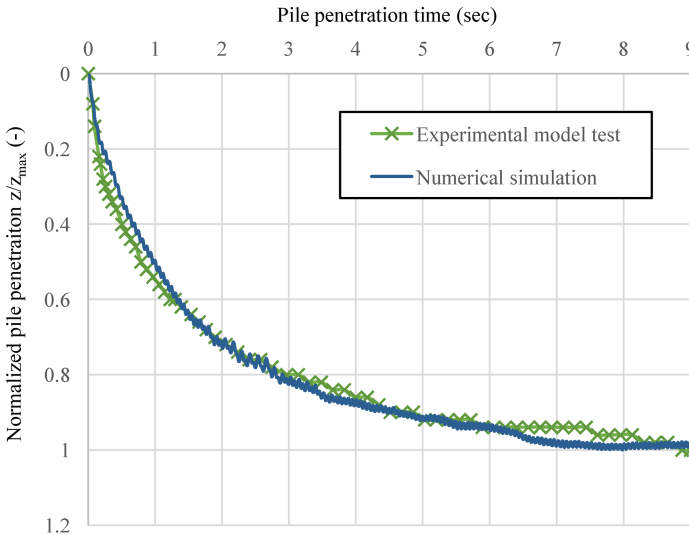


Fig. 4. Normalized model pile penetration z/z_{\max} vs. time: experimental model test measurements and numerical simulation results

To investigate the pile buckling behavior during vibratory installation with 23 Hz under different conditions the elastic-plastic pile was first numerically penetrated into the homogeneous model (Fig. 3) for about 8 s, which corresponds to 0.65 m penetration. No pile buckling or large deformations occurred until this penetration depth. The vertical stress contours in the soil during vibratory penetration are shown in Fig. 5. Six different time steps from 6.29 to 6.34 s were selected, corresponding to slightly more than one cycle of sinusoidal frequency loading (Fig. 5a).

For results interpretation the evaluation criteria are mean strain, internal energy, pile vertical displacement, and pile lateral (horizontal) displacement. The mean strain is calculated as one-third of the strain tensor trace and defined based on the infinitesimal theory. The internal energy is the work done to induce strain in a unit volume of the solid part which can be used here to evaluate the accumulated strain in the pile during

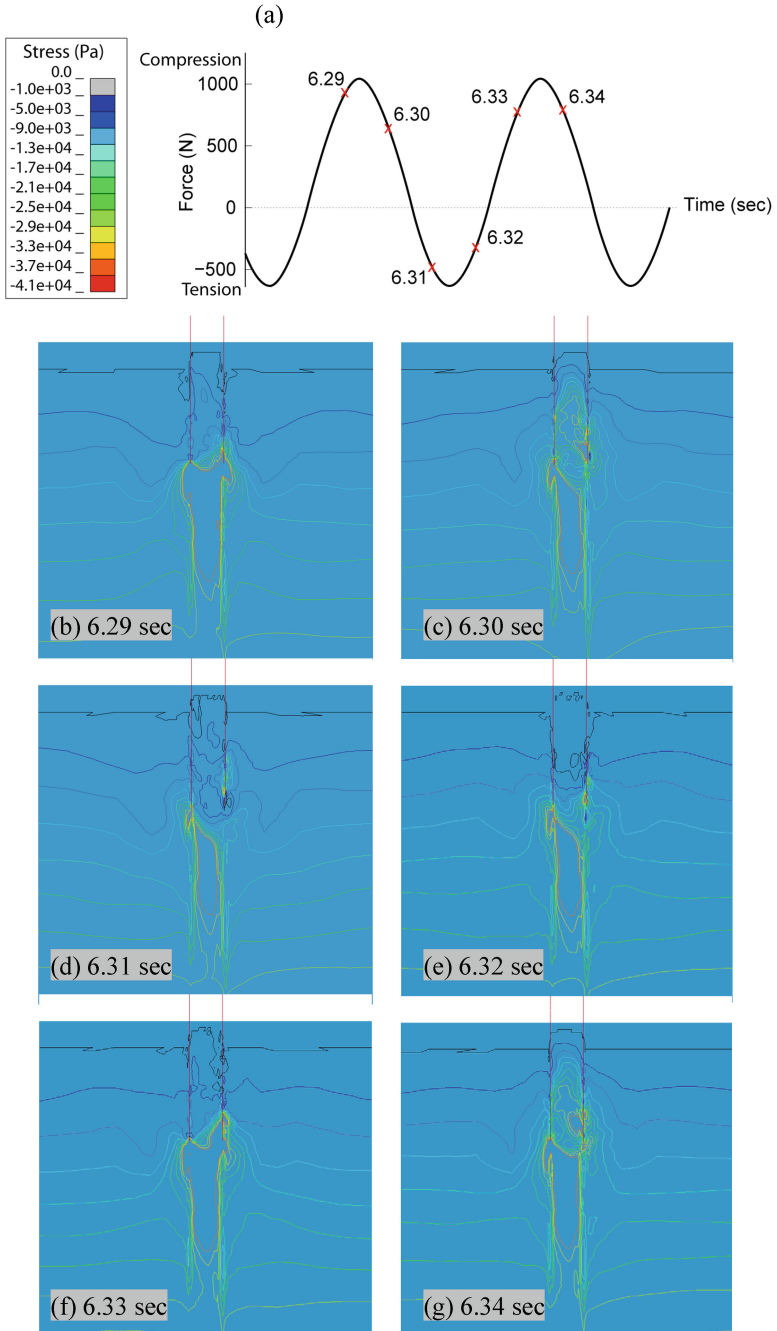


Fig. 5. Vibratory loading function (a) and isolines of induced vertical stresses in the soil at different times during one vibration cycle (b) to (g)

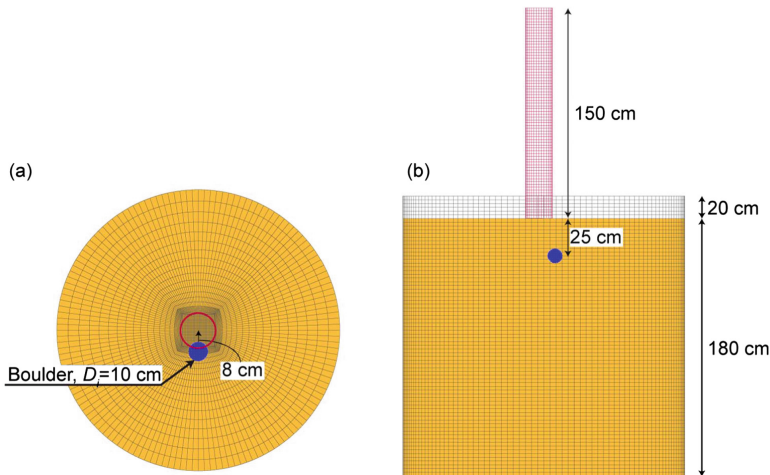


Fig. 6. FE model of pipe pile installation containing a boulder in the soil: (a) planar, (b) side view [12]

installation. The horizontal displacement is obtained by averaging the nodal displacements of all nodes in the pile.

Figure 7 shows results from the four models (ovality, flatness, and straightness of the pile, as well as boulder heterogeneity in the soil as shown in Fig. 6) in comparison to the initial reference model containing homogeneous soil and a perfectly shaped pile (Fig. 3).

The pile in the reference model penetrated until 0.65 m at 8 s vibration time without suffering any significant strain. Although the detailed evaluation of strain is not shown here, the beginning of slight deformations is recognizable from the internal energy (Fig. 7 bottom).

The internal energy in the reference model started to increase at about 7.2 s vibration time, which corresponds to a penetration depth of about 0.63 m (Fig. 7 top). In the other four models, the final penetration is much less compared to the reference model. The boulder in the soil influences the penetration rate most, leading to only about 0.3 m penetration after 8 s vibration.

From the evolution of internal energy with pile vibration time it can be seen (Fig. 7 bottom), that the trend of the internal energy curves corresponds to the deviation of the penetration curves (vertical displacement, Fig. 7 top) from the reference model. That means the energy starts to increase substantially if the pile begins to exhibit accumulation of strains and buckling phenomena (the curves in Fig. 7 (bottom) are cut to a value of 42 J). This interdependency follows from the fact, that the same driving force was used for all models. Therefore the same energy is applied to all the piles and according to the energy conservation law, the driving energy must have been spent on other phenomena such as lateral displacements, additional strains and/or buckling in a pile.

Consequently the evolution of the horizontal pile displacement with time (Fig. 7 middle) correlates in general also with the before mentioned behavior. But the lateral

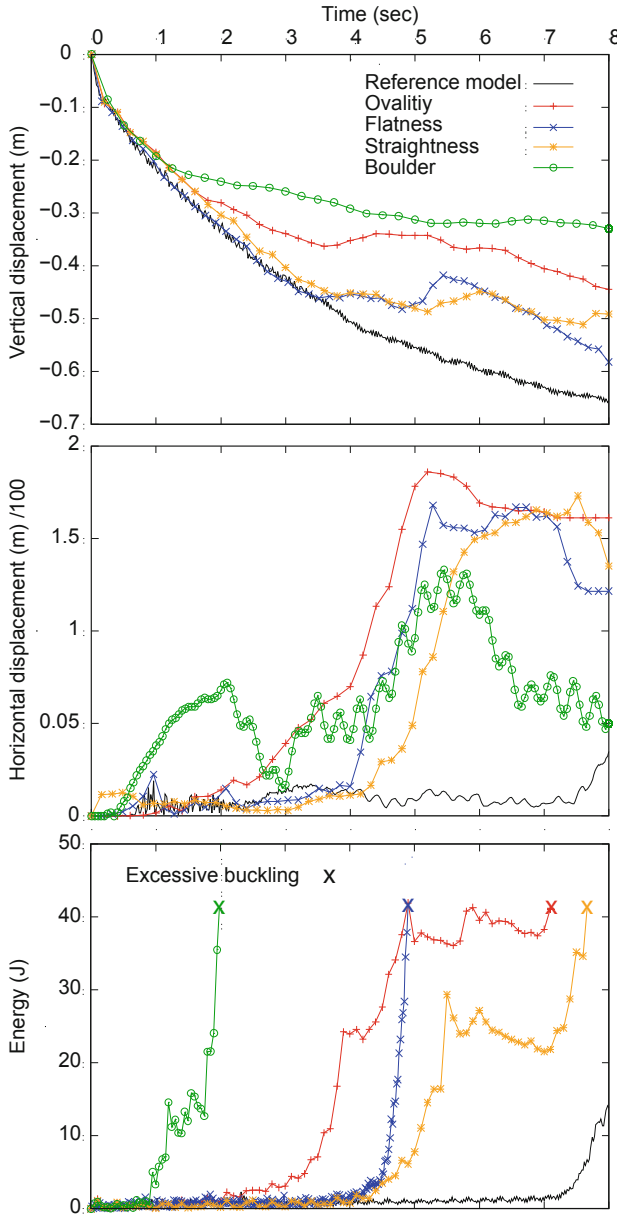


Fig. 7. Influence of pile imperfections and soil heterogeneity on pile penetration behavior: (top) vertical pile displacement, (middle) horizontal pile displacement, and (bottom) internal energy [12]

pile displacement is limited and maintained after some penetration due to the resistance of the surrounding soil. Thus, the remaining driving energy must have been spent on

buckling and/or large deformation. In some cases a decrease in the internal energy value is observed after significant grow, which can be related to induced elastic strains in the pile and a kind of elastically pile spring back movement due to further penetration. This phenomenon was also supposed by Aldridge et al. [15].

Figure 8 shows the pile shape due to deformation of each analyzed model. The deformed shapes are evaluated at the time where the internal energy reached a maximum. Also plotted is the mean infinitesimal strain as contour plot on the deformed shape of the piles at the same time step. With the exception of the reference model, all other models show significant large deformation of the pile. This deformation is greatest at the pile tip. At the pile tip is the mean strain also the largest. Therefore this phenomenon in engineering practice is often referred to “pile tip buckling”. The buckling and potential damage of the pile starts to evolve from the tip.

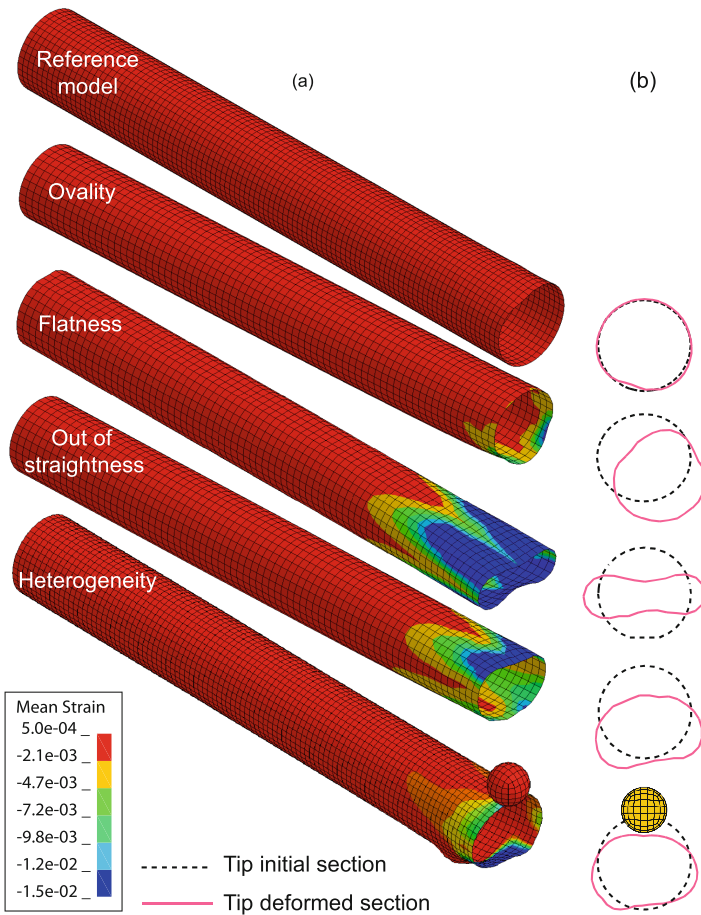


Fig. 8. (a) Deformed pile shape and mean infinitesimal strain at the time steps with maximum internal energy and (b) cross section shapes of the pile tips [12]

The amount of large deformation depends on the initial imperfection of the pile and the heterogeneity of the soil respectively. Each pile shows a different buckling mode due to the different initial imperfection. The largest pile tip deformation occurs with an initially flat pile. It is also interesting to note, that the deformed pile shape becomes non-symmetric with further penetration. It can be observed from the numerical results (Fig. 8b), that the cross section shapes of the tips of the imperfect piles tend to take the forms of the so-called “peanut-shape” as reported also in the literature [15].

It can be assumed that the proposed numerical model covers the complex pile-soil interaction behavior during dynamic installation of open-ended tubular piles quite well. Phenomena and boundary conditions like soil resistance, pile imperfection, and heterogeneity are included therein.

3.2 Sand Column Collapse

The controlled outflow of a defined volume of sand out of a hollow cylinder or container is a common laboratory experiment to investigate fundamental granular flow phenomena and behavior. This experiment is also called sand column collapse in the literature [16, 17].

The general experimental set-up is shown in Fig. 9 left. A column of sand is held in rest inside a rectangular container. The holding gate or wall is suddenly uplifted allowing the sand to collapse and flow out by its own weight. The investigations performed by Lube et al. [16] are used as an experimental reference to analyze and to validate own numerical ALE models.

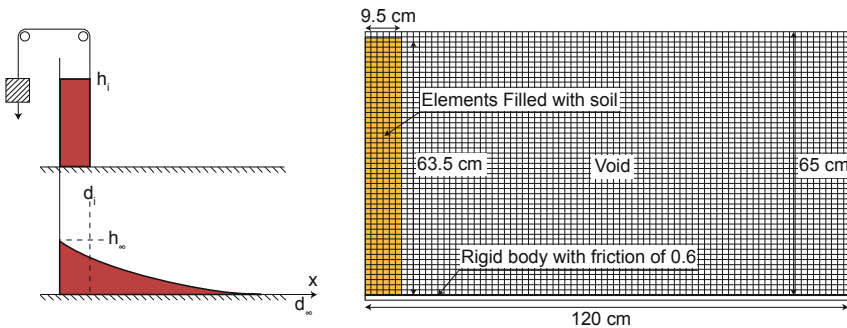


Fig. 9. Experimental set-up (left) and numerical ALE model in LS-Dyna (right) of the sand collapse problem [18]

The left hand side wall of the experimental set-up is considered to be a symmetry condition in the numerical model. Initial dimensions of the soil column are: width 9.5 cm, height 65 cm and depth 20 cm in direction normal to flow.

Two different constitutive models are used to represent the soil behavior. First a simple Mohr-Coulomb relation and second an advanced hypoplastic model. The hypoplastic model parameters are estimated to fit the Mohr-Coulomb parameters using numerical simulations of triaxial tests. This procedure and the resulting model parameters are given in Bakroon et al. [18].

In the 3D finite element model single point reduced integration elements with 15 mm element size are used. To achieve a plane strain condition one element in depth direction was modeled. A void region is defined to let the soil material flow to these void elements after the sand solumn collapse initiates. The container is modeled as a frictionless rigid body part which is removed as the initial stresses are initialized. Gravity acceleration is assigned with 9.806 m/s^2 in order to calculate the initial stresses. The modeled surface friction (penalty contact) of the rigid body at the bottom where the sand runs along is taken equal to the internal friction of the sand. Sand solumn collapse is initiated by abruptly lifting up one side of the rectangular container. The total calculation time of the problem is 2 s only.

In Fig. 10 the sand surface evolution and run-out distances with time are shown. Although all simulations give acceptable results in comparison with the experiment, the best fit is obtained when using a hypoplastic soil model in connection with the MMALE numerical model. Both the run-out distances and the heights of the sand slope with time are best predicted by hypoplasticity compared to the simple Mohr-Coulomb model. The worst result compared to the experiment is achieved using the CEL approach in conjunction with the Mohr-Coulomb model.

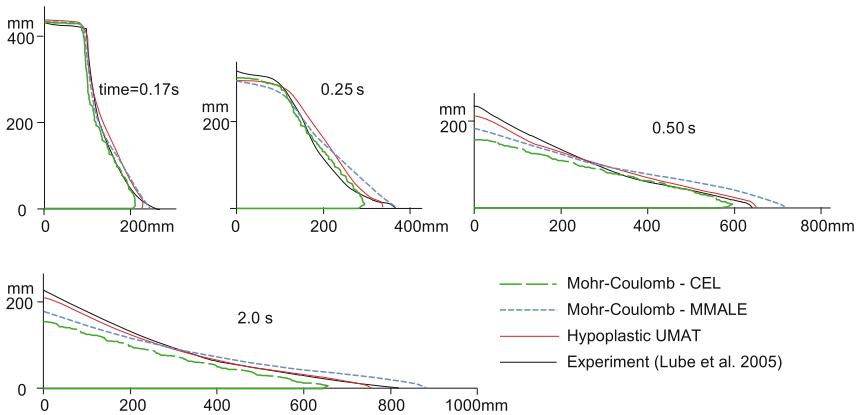


Fig. 10. Sand surface evolution with time: comparison of numerical results with the sand solumn collapse experiment

A fair judgment between the different ALE models is to compare CEL with MMALE by using the same simple Mohr-Coulomb model. The CEL simulation underpredicts the sand surface at any time step, whereas the MMALE simulation is closer to the surface measured in the experiment, but after some distance from the container it predicts a higher surface and longer run-out distance than in the experiment. The difference in the predicted run-out distance between CEL and MMALE is about 200 mm with the experiment being closer to the MMALE result.

Another interesting results evaluation concerns the void ratio distribution calculated with the hypoplastic MMALE numerical model, which is presented in Fig. 11 at various times. The initial void ratio was 0.695 before the sand solumn collapse started.

The minimum and maximum void ratios of the modeled sand are 0.55 and 0.95 respectively. Right after the collapse was initiated the void ratio tends to increase, only at the bottom and inside the core of the sand column there is the initial void ratio kept. This core of the column is compacted in the following time but its expansion size remains almost constant during the entire analysis.

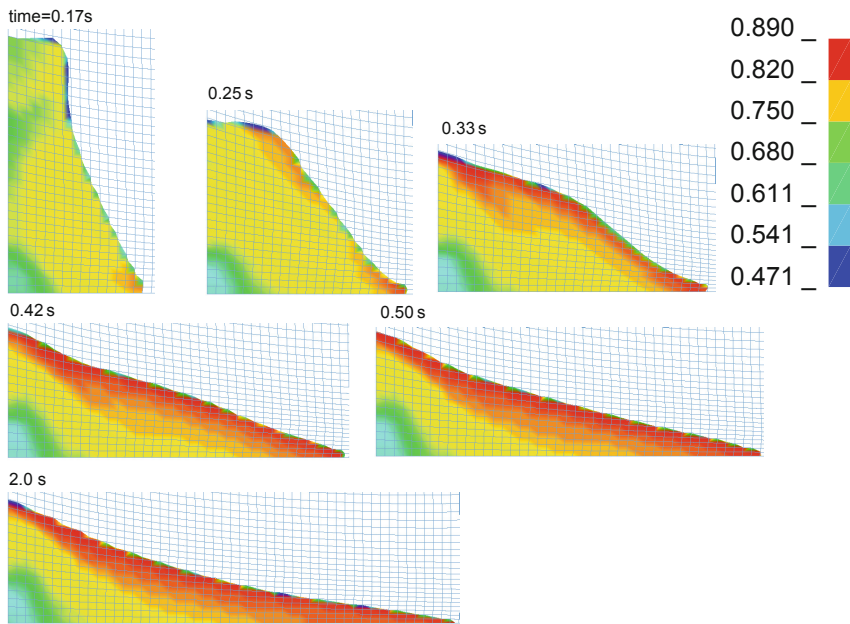


Fig. 11. MMALE with hypoplastic soil model: void ratio distribution at various times of the simulation.

The top sand layers exhibit loosening behavior (red color in Fig. 11), but do not reach the maximum void ratio of the sand. Finally at the end of the flow process a clearly visible three layered structure of the sand mass is achieved, with a dense core, a medium dense middle part (yellow color in Fig. 11) and a loose top layer. The void ratio distribution in the results must be further evaluated to demonstrate whether the change of void ratio over the height is continuous or not.

The interpretation of the void ratio at the surface has to be done with special care. Due to the presence of the void elements outside the sand volume the void ratio contour values are averaged void ratio values for mixed elements containing soil and void. Since void ratio of the void elements is always zero, the resulting averaged void ratio is not the real void ratio of the soil.

A detailed comparison of the CEL and the MMALE models is shown in Figs. 12 and 13. The final shape of the sand surface as well as the interface details at the end of the flow process highlight the difference between CEL and MMALE models (Fig. 12). The fixed Eulerian mesh in the CEL model leads to a rough surface reconstruction,

illustrated by means of the plotted volume fraction contours. It results in a stronger numerical diffusion in the CEL simulation, which can also explain the shorter run-out distance from this analysis compared to MMALE.

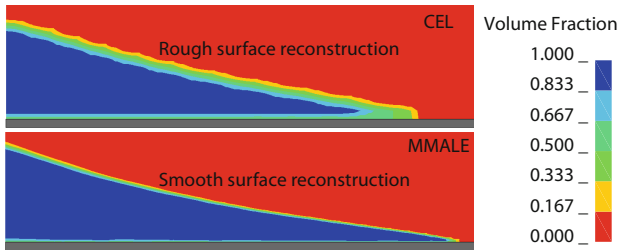


Fig. 12. Contour plot of volume fraction from CEL (top) and MMALE (bottom) analyses at final run-out of the sand mass [4]

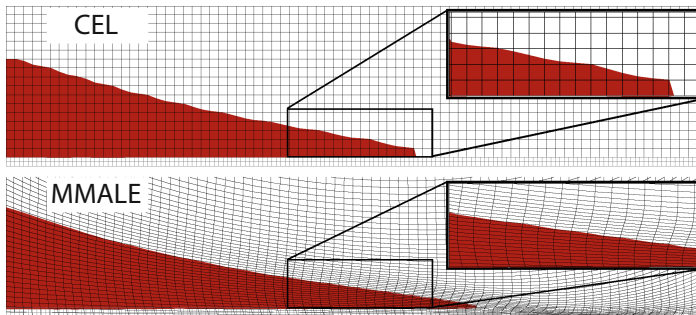


Fig. 13. Shape of material and mesh from CEL (top) and MMALE (bottom) analyses at final run-out of the sand mass [4]

The smoother surface reconstruction is also clearly visible in Fig. 13 (bottom). MMALE is capable of doing a much smoother surface reconstruction compared to CEL due to the mesh update algorithms. Of course one can achieve a smoother surface with CEL too, but that requires a finer mesh in the whole discretized domain, leading to much higher computational costs.

4 Summary and Conclusions

The performance of ALE methods is evaluated by means of two application examples: the vibratory driven installation of open-ended tubular steel piles in sand and the sand column collapse problem. The MMALE soil-pile interaction model provides reliable measures to assess pile buckling. As a result from this pile buckling analyses it can be argued that the driving energy for the pile installation is reflected in the model mainly

in three different forms: vertical and horizontal pile displacement, and pile buckling. Overall it can be concluded that the proposed numerical model covers the complex soil-pile interaction behavior during dynamic installation of open-ended tubular piles quite well. Phenomena and boundary conditions like soil resistance, pile imperfections, and heterogeneity are included therein.

From the second application, the sand column collapse, different results from two constitutive models as well as two ALE approaches are gained. The latter comparison proves the advantage of MMALE with much smoother surface reconstruction compared to CEL due to the mesh update algorithms in MMALE with less computational costs.

All simulation results assess the feasibility of ALE methods in geotechnical large deformation problems, concluding that the ALE method is a promising framework for the solution of complex large deformation problems in geotechnical engineering.

Acknowledgments. The author is grateful for carrying out the numerical analysis and preparation of figures by Montaser Bakroon and Reza Daryaei. Special thanks to Daniel Aubram for countless discussions over the years, not only about the ALE methods. Last but not least, the author would like to acknowledge his highly esteemed colleague Prof. Dr.-Ing. habil. Theodoros Triantafyllidis for numerous inspiring and creative discussions in joint research projects of the past years - thank you very much!

References

1. Beuth, L., Benz, T., Vermeer, P.A., Coetzee, C.J., Bonnier, P., van den Berg, P.: Formulation and validation of a quasi-static Material Point Method. In: Numerical Models in Geomechanics: Proceedings of the 10th International Symposium on Numerical Models in Geomechanics (NUMOG X), Rhodes, Greece, 25–27 April 2007 (2007)
2. Bui, H.H., Fukagawa, R., Sako, K.: Smoothed particle hydrodynamics for soil mechanics. In: Numerical Methods in Geotechnical Engineering, pp. 275–281 Taylor & Francis Group, London (2006)
3. Benson, D.J.: An efficient, accurate, simple ALE method for nonlinear finite element programs. *Comput. Methods Appl. Mech. Eng.* **72**(3), 305–350 (1989)
4. Bakroon, M., Daryaei, R., Aubram, D., Rackwitz, F.: Investigation of mesh improvement in multi-material ALE formulations for large deformation problems. *Int. J. Geomech. ASCE* (2019, submitted)
5. Qiu, G., Henke, S., Grabe, J.: Application of a Coupled Eulerian-Lagrangian approach on geomechanical problems involving large deformations. *Comput. Geotech.* (2011). <https://doi.org/10.1016/j.compgeo.2010.09.002>
6. Qiu, G., Henke, S.: Controlled installation of Spudcan foundations on loose sand overlying weak clay. *Marine Structures* (2011). <https://doi.org/10.1016/j.marstruc.2011.06.005>
7. Tho, K.K., Leung, C.F., Chow, Y.K., Swaddiwudhipong, S.: Eulerian finite-element technique for analysis of Jack-Up Spudcan Penetration. *Int. J. Geomech. ASCE* (2012). [https://doi.org/10.1061/\(ASCE\)GM.1943-5622.0000111](https://doi.org/10.1061/(ASCE)GM.1943-5622.0000111)
8. Hamann, T., Qiu, G., Grabe, J.: Application of a Coupled Eulerian-Lagrangian approach on pile installation problems under partially drained conditions. *Comput. Geotech.* (2014). <https://doi.org/10.1016/j.compgeo.2014.10.006>

9. Di, Y., Yang, J., Sato, T.: An operator-split ALE method for large deformation analysis of geomaterials. *Int. J. Numer. Anal. Meth. Geomech.* (2007). <https://doi.org/10.1002/nag.601>
10. Aubram, D., Rackwitz, F., Wriggers, P., Savidis, S.A.: An ALE method for penetration into sand utilizing optimization-based mesh motion. *Comput. Geotech.* (2015). <https://doi.org/10.1016/j.compgeo.2014.12.012>
11. Aubram, D., Rackwitz, F., Savidis, S.A.: Contribution to the Non-Lagrangian formulation of geotechnical and geomechanical processes. In: Triantafyllidis, T. (ed.) *Holistic Simulation of Geotechnical Installation Processes – Theoretical Results and Applications*. LNACM, vol. 82. Springer, Heidelberg (2017). https://doi.org/10.1007/978-3-319-52590-7_3
12. Bakroon, M., Daryaei, R., Aubram, D., Rackwitz, F.: Numerical evaluation of buckling in steel pipe piles during vibratory installation. *Soil Dyn. Earth. Eng.* (2019). <https://doi.org/10.1016/j.soildyn.2018.08.003>
13. Winslow, A.M.: Equipotential zoning of two-dimensional meshes (UCRL-7312). United States (1963)
14. van Leer, B.: Towards the ultimate conservative difference scheme. *J. Comput. Phys.* (1997). <https://doi.org/10.1006/jcph.1997.5704>
15. Aldridge, T.R., Carrington, T.M., Kee, N.R.: Propagation of pile tip damage during installation. *Frontiers in offshore geotechnics*. In: *Proceedings of the 1st International Symposium on Frontiers in Offshore Geotechnics, ISFOG 2005*, p. 823-7 (2005)
16. Lube, G., Huppert, H.E., Sparks, R.S.J., Freundt, A.: Collapses of two-dimensional granular columns. *Phys. Rev. E* (2005). <https://doi.org/10.1103/PhysRevE.72.041301>
17. Thompson, E.L., Huppert, H.E.: Granular column collapses: further experimental results. *J. Fluid Mech.* (2007) <https://doi.org/10.1017/S0022112006004563>
18. Bakroon, M., Daryaei, R., Aubram, D., Rackwitz, F.: Implementation and validation of an advanced hypoplastic model for granular material behavior. In: *Proceedings of the 15th International LS-DYNA Users Conference* (2018). <https://www.dynalook.com/conferences/15th-international-ls-dyna-conference>